

Influence of the Earth Rotation on Trajectory of a Returnable Hypersonic Cruise Vehicle

*Kaiqiang Wang, Yanze Hou and Chong Chen

China Academy of Space Technology, Beijing 100094, China

* wangkaiqiang1988@163.com

Abstract. It is of high difficulty for a hypersonic vehicle to implement a hypersonic cruise flight and return to a scheduled airport without power. Accuracy of mission simulation and analysis is more crucial at this time. Under this circumstance, it is meaningful to discuss whether the earth rotation should be considered in the dynamic model and trajectory design. In this research, the dynamic equations in which the earth rotation is taken into consideration are derived for a hypersonic cruise vehicle. The direct shooting method is utilized for parameterization and discretization of the trajectory, so that the trajectory can be analyzed and simulated through numerical integration. Then, two groups of trajectory simulation results are presented. In each group, the only difference between the two trajectories is that whether the earth rotation is involved, and the two trajectories are compared with each other. For a returnable hypersonic cruise vehicle which returns to the ground without power, whether to involve the earth rotation in the dynamic model is discussed on the basis of the numerical results, and relevant suggestions are given for reference.

1. Introduction

Along with the development of the scramjet, the hypersonic cruise vehicle has been attracting more and more attention. With the use of scramjet, it has better propulsive efficiency and can cruise above the altitude of 20 km with a Mach number larger than 5. After the cruise phase, it can descent without any power until it finally lands at the scheduled airport. Due to its highly fast cruise speed and reusability, the hypersonic cruise vehicle has great potentials in two-stage-to-orbit (TSTO) launch vehicles [1]. Until now, only the US has successfully implemented a few X-43 hypersonic flight tests, in which the hypersonic cruise lasts more than 10s and the Mach number exceeds 7 [2]. However, X-43 was finally controlled to fall into the ocean instead of returning back to the ground.

In the trajectory related researches, some take the earth rotation into consideration, while the others don't. Without considering the earth rotation, Roh and Kim studied on trajectory optimization for a multi-stage launch vehicle [3]; Grant and Braun implemented unpowered trajectory optimization for a hypersonic flight [4]; Manickavasagam et al. optimized the trajectory for long range and air-to-air tactical flight vehicles [5]. As to the reentry trajectory design and optimization, some researches involve the earth rotation into the dynamic model [6-8], while some others don't take it into account [9]. Generally speaking, whether to consider the earth rotation depends on the mission objective, the flight phase considered, total flight range and the landing precision needed in a specific trajectory problem.

However, there are few researches on the similar topic for a returnable hypersonic cruise vehicle. This paper aims to study on the influence of the earth rotation on trajectory and to discuss whether to



involve the earth rotation in the dynamic model for the hypersonic cruise vehicle. After the powered climb and cruise phases, it descends and returns to the ground without power. In Section 2, the dynamic equations are derived based on a few basic coordinate systems, and the dynamic model is established in which the earth rotation is taken into account. Section 3 briefly introduces the direct shooting method for parameterization and discretization of the trajectory. In Section 4, two groups of trajectory simulation results are presented, and relevant comparisons and discussions are made with respect to the effects of earth rotation. In Section 5, the research is summarized and suggestions are given.

2. Dynamics modeling

2.1. Coordinates

Five coordinates are used in this paper.

2.1.1. Geocentric coordinate system $O_E - x_E y_E z_E$. The origin O_E is located at the geocenter, axis $O_E x_E$ is in the equator and points to the Greenwich meridian, $O_E z_E$ points to the North Pole, and $O_E y_E$ is determined according to the right-hand rule. The coordinate is fixed with the earth and rotates with it.

2.1.2. Azimuth coordinate system $O_1 - x_A y_A z_A$. The origin O_1 is located at the instantaneous mass center of hypersonic vehicle, axis $O_1 x_A$ is in the local horizontal plane and points to the North Pole, $O_1 y_A$ is perpendicular to the horizontal plane and is straight up, and $O_1 z_A$ is determined according to the right-hand rule which points to the east.

2.1.3. Ground coordinate system $O_G - x_G y_G z_G$. The origin O_G is located at the intersection of the line from the geocenter to O_1 and the ground surface of the earth, axis $O_G x_G$ is in the horizontal plane which contains O_G and points to the direction of the projection of the ground velocity vector \mathbf{v} on this horizontal plane, $O_G y_G$ is perpendicular to this horizontal plane and is straight up, and $O_G z_G$ is given according to the right-hand rule.

2.1.4. Body coordinate system $O_1 - x_b y_b z_b$. The origin O_1 is the instantaneous mass center of hypersonic vehicle as explained above, $O_1 x_b$ is along the vertical axis of the hypersonic vehicle and points to its nose, $O_1 y_b$ is in its vertical symmetry plane which is perpendicular to $O_1 x_b$ and sticks straight up, and $O_1 z_b$ is determined according to the right-hand rule. The coordinate is fixed with the hypersonic vehicle.

2.1.5. Trajectory coordinate system $O_1 - x_T y_T z_T$. The origin O_1 is the instantaneous mass center of the vehicle as explained above, $O_1 x_T$ is along the direction of the ground velocity vector \mathbf{v} , axis $O_1 y_T$, perpendicular to $O_1 x_T$, is located in the vertical plane containing the vector \mathbf{v} and sticks straight up, and $O_1 z_T$ is given according to the right-hand rule.

2.2. Coordinate transformations

In this paper, only motion of the hypersonic vehicle in the vertical plane is considered. Then, the following four coordinate transformations are needed.

2.2.1. From geocentric coordinate system to azimuth coordinate system. The direction cosine matrix C_{AE} is obtained through 3 coordinate transformations:

$$\begin{aligned}
C_{AE} &= C_z(-\delta)C_y(-90^\circ)C_z(\lambda-90^\circ) \\
&= \begin{bmatrix} \cos(-\delta) & \sin(-\delta) & 0 \\ -\sin(-\delta) & \cos(-\delta) & 0 \\ 0 & 0 & 1 \end{bmatrix} \begin{bmatrix} \cos(-90^\circ) & 0 & -\sin(-90^\circ) \\ 0 & 1 & 0 \\ \sin(-90^\circ) & 0 & \cos(-90^\circ) \end{bmatrix} \begin{bmatrix} \cos(\lambda-90^\circ) & \sin(\lambda-90^\circ) & 0 \\ -\sin(\lambda-90^\circ) & \cos(\lambda-90^\circ) & 0 \\ 0 & 0 & 1 \end{bmatrix} \\
&= \begin{bmatrix} -\cos \lambda \sin \delta & -\sin \lambda \sin \delta & \cos \delta \\ \cos \lambda \cos \delta & \sin \lambda \cos \delta & \sin \delta \\ -\sin \lambda & \cos \lambda & 0 \end{bmatrix}
\end{aligned} \tag{1}$$

where δ and λ are latitude and longitude of the hypersonic vehicle, respectively.

2.2.2. From azimuth coordinate system to trajectory coordinate system. The direction cosine matrix C_{TA} is given based on the velocity azimuth A_z as well as the flight-path angle γ :

$$\begin{aligned}
C_{TA} &= C_z(\gamma)C_y(-A_z) \\
&= \begin{bmatrix} \cos \gamma & \sin \gamma & 0 \\ -\sin \gamma & \cos \gamma & 0 \\ 0 & 0 & 1 \end{bmatrix} \begin{bmatrix} \cos A_z & 0 & \sin A_z \\ 0 & 1 & 0 \\ -\sin A_z & 0 & \cos A_z \end{bmatrix} \\
&= \begin{bmatrix} \cos \gamma \cos A_z & \sin \gamma & \cos \gamma \sin A_z \\ -\sin \gamma \cos A_z & \cos \gamma & -\sin \gamma \sin A_z \\ -\sin A_z & 0 & \cos A_z \end{bmatrix}
\end{aligned} \tag{2}$$

2.2.3. From ground coordinate system to trajectory coordinate system. The direction cosine matrix C_{TG} is acquired through one coordinate transformation based on the flight-path angle γ :

$$C_{TG} = C_z(\gamma) = \begin{bmatrix} \cos \gamma & \sin \gamma & 0 \\ -\sin \gamma & \cos \gamma & 0 \\ 0 & 0 & 1 \end{bmatrix} \tag{3}$$

2.2.4. From body coordinate system to trajectory coordinate system. The direction cosine matrix C_{TB} is obtained based on the angle of attack α , in which sideslip angle is maintained to zero all the time:

$$C_{TB} = C_z(-\alpha) = \begin{bmatrix} \cos(-\alpha) & \sin(-\alpha) & 0 \\ -\sin(-\alpha) & \cos(-\alpha) & 0 \\ 0 & 0 & 1 \end{bmatrix} \tag{4}$$

2.3. Dynamic equations

It is worth noting that only motion of the hypersonic vehicle in the vertical plane is considered in this paper. According to Newtonian mechanics, the absolute derivative of the ground velocity vector \mathbf{v} with respect to time t is given by the following equation, in which the convected acceleration and Coriolis acceleration are taken into account:

$$\frac{d\mathbf{v}}{dt} = \left(\frac{\partial \mathbf{v}}{\partial t} + \boldsymbol{\omega}_{TG} \times \mathbf{v} \right) + \boldsymbol{\omega}_e \times (\boldsymbol{\omega}_e \times \mathbf{r}) + 2\boldsymbol{\omega}_e \times \mathbf{v} = \frac{\mathbf{F}}{m} + \mathbf{g} \tag{5}$$

where m is the mass of the vehicle, $\partial \mathbf{v} / \partial t$ is the relative derivative of the vector \mathbf{v} in the trajectory coordinate system, $\boldsymbol{\omega}_{TG}$ is the rotational angular velocity of the trajectory coordinate compared to the

geocentric coordinate system, $\boldsymbol{\omega}_e$ is the angular velocity vector of the earth rotation, \mathbf{r} is the distance vector from the geocenter to the mass center of the vehicle, \mathbf{F} represents the external force vector acting on the hypersonic vehicle, and \mathbf{g} is the gravitational acceleration vector.

2.3.1. *Differential of the ground velocity vector \mathbf{v} .* In the trajectory coordinate system, $\boldsymbol{\omega}_{TG}$ is described as

$$\boldsymbol{\omega}_{TG}^T = C_{TA} C_z(-\delta) C_y(-90^\circ) \begin{bmatrix} 0 \\ 0 \\ \dot{\lambda} \end{bmatrix} + C_{TA} \begin{bmatrix} 0 \\ 0 \\ \dot{\delta} \end{bmatrix} + C_{TG} \begin{bmatrix} 0 \\ -\dot{A}_z \\ 0 \end{bmatrix} + \begin{bmatrix} 0 \\ 0 \\ \dot{\gamma} \end{bmatrix} \quad (6)$$

The derivatives of latitude δ and longitude λ with respect to time t are as follows:

$$\frac{d\lambda}{dt} = \frac{v \cos \gamma \sin A_z}{(r_e + h) \cos \delta} \quad (7)$$

$$\frac{d\delta}{dt} = \frac{v \cos \gamma \cos A_z}{(r_e + h)} \quad (8)$$

where v is the flight speed, r_e is the radius of the earth, and h is the altitude of the vehicle. Then, in the trajectory coordinate system:

$$\frac{\partial \mathbf{v}}{\partial t} + \boldsymbol{\omega}_{TG} \times \mathbf{v} = \begin{bmatrix} \dot{v} \\ 0 \\ 0 \end{bmatrix} + \boldsymbol{\omega}_{TG}^T \times \begin{bmatrix} v \\ 0 \\ 0 \end{bmatrix} = \begin{bmatrix} \frac{dv}{dt} \\ v \frac{d\gamma}{dt} - \frac{v^2 \cos \gamma}{r_e + h} \\ -v \cos \gamma \frac{dA_z}{dt} + \frac{v^2 \cos^2 \gamma \tan \delta \sin A_z}{r_e + h} \end{bmatrix} \quad (9)$$

2.3.2. *The convected acceleration.* It is first expressed in the azimuth coordinate system, and then is transformed in the trajectory coordinate:

$$\begin{aligned} \boldsymbol{\omega}_e \times (\boldsymbol{\omega}_e \times \mathbf{r}) &= C_{TA} \begin{bmatrix} \sin \delta \\ -\cos \delta \\ 0 \end{bmatrix} \omega_e^2 (r_e + h) \cos \delta \\ &= \begin{bmatrix} \sin \delta \cos \gamma \cos A_z - \cos \delta \sin \gamma \\ -\sin \delta \sin \gamma \cos A_z - \cos \delta \cos \gamma \\ -\sin \delta \sin A_z \end{bmatrix} \omega_e^2 (r_e + h) \cos \delta \end{aligned} \quad (10)$$

2.3.3. *Coriolis acceleration.* The angular velocity vector of the earth rotation $\boldsymbol{\omega}_e$ is firstly transformed from the geocentric coordinate to the trajectory coordinate as

$$\boldsymbol{\omega}_e^T = C_{TA} C_{AE} \begin{bmatrix} 0 \\ 0 \\ \boldsymbol{\omega}_e \end{bmatrix} = \begin{bmatrix} \cos \delta \cos \gamma \cos A_z + \sin \delta \sin \gamma \\ -\cos \delta \sin \gamma \cos A_z + \sin \delta \cos \gamma \\ -\cos \delta \sin A_z \end{bmatrix} \boldsymbol{\omega}_e \quad (11)$$

Then, in the trajectory coordinate system, the Coriolis acceleration is formulated as

$$2\boldsymbol{\omega}_e \times \mathbf{v} = 2\boldsymbol{\omega}_e^{T \times} \begin{bmatrix} v \\ 0 \\ 0 \end{bmatrix} = 2\boldsymbol{\omega}_e v \begin{bmatrix} 0 \\ -\cos \delta \sin A_z \\ \cos \delta \sin \gamma \cos A_z - \sin \delta \cos \gamma \end{bmatrix} \quad (12)$$

2.3.4. *The external force vector \mathbf{F} .* As thrust vector control is excluded in this paper, the thrust is always along the direction of axis O_1x_b . Thus, in the trajectory coordinate system:

$$\mathbf{F}^T = C_{TB} \begin{bmatrix} F_t \\ 0 \\ 0 \end{bmatrix} + \begin{bmatrix} -D \\ L \\ 0 \end{bmatrix} = \begin{bmatrix} F_t \cos \alpha - D \\ F_t \sin \alpha + L \\ 0 \end{bmatrix} \quad (13)$$

where F_t is the thrust, D and L are aerodynamic drag and lift, respectively, calculated as follows:

$$\begin{cases} D = q_d S_r C_D \\ L = q_d S_r C_L \end{cases} \quad (14)$$

In the above equation, q_d is the dynamic pressure, S_r is the aerodynamic reference area, C_D and C_L are drag and lift coefficients, respectively. The dynamic pressure is given by

$$q_d = \frac{1}{2} \rho v^2 \quad (15)$$

where ρ is the atmospheric density.

2.3.5. *The gravitational acceleration vector \mathbf{g} .* In the trajectory coordinate system, the vector is described as

$$\mathbf{g}^T = C_{TG} \begin{bmatrix} 0 \\ -g \\ 0 \end{bmatrix} = \begin{bmatrix} \cos \gamma & \sin \gamma & 0 \\ -\sin \gamma & \cos \gamma & 0 \\ 0 & 0 & 1 \end{bmatrix} \begin{bmatrix} 0 \\ -g \\ 0 \end{bmatrix} = \begin{bmatrix} -g \sin \gamma \\ -g \cos \gamma \\ 0 \end{bmatrix} \quad (16)$$

where g is the gravitational acceleration.

2.3.6. *Additional equations.* The following additional equations are needed in the meantime:

$$\frac{dm}{dt} = -m_c \quad (17)$$

$$\frac{dh}{dt} = v \sin \gamma \quad (18)$$

In equation (17), m_c is the mass flow of engine.

2.3.7. *The summarized dynamic equations.* The dynamic equations are finally shown as follows. The angle of attack α is the only control variable, whilst v , γ , A_z , m , h , λ and δ constitute the state variables.

$$\left\{ \begin{array}{l}
\frac{dv}{dt} = \frac{(F_t \cos \alpha - D)}{m} - g \sin \gamma + \omega_e^2 (r_e + h) \cos \delta \times (\cos \delta \sin \gamma - \sin \delta \cos \gamma \cos A_z) \\
\frac{d\gamma}{dt} = \frac{(F_t \sin \alpha + L)}{mv} + \left(\frac{v}{r_e + h} - \frac{g}{v} \right) \cos \gamma + \frac{\omega_e^2 (r_e + h) \cos \delta}{v} (\cos \delta \cos \gamma + \sin \delta \sin \gamma \cos A_z) \\
\quad + 2\omega_e \cos \delta \sin A_z \\
\frac{dA_z}{dt} = \frac{v \cos \gamma}{r_e + h} \tan \delta \sin A_z + \frac{\omega_e^2 (r_e + h) \cos \delta \sin \delta \sin A_z}{v \cos \gamma} + 2\omega_e (\sin \delta - \cos \delta \tan \gamma \cos A_z) \\
\frac{dm}{dt} = -m_c \\
\frac{dh}{dt} = v \sin \gamma \\
\frac{d\lambda}{dt} = \frac{v \cos \gamma \sin A_z}{(r_e + h) \cos \delta} \\
\frac{d\delta}{dt} = \frac{v \cos \gamma \cos A_z}{(r_e + h)}
\end{array} \right. \quad (19)$$

2.4. Geophysical Model of the Earth

2.4.1. *Gravity model.* To describe the gravitational acceleration and radius of the earth, the J2 gravity model is used here:

$$g = \frac{\mu_e}{(r_e + h)^2} + \frac{3J_2 r_a^2 \mu_e (1 - 3 \sin^2 \delta)}{2(r_e + h)^4} \quad (20)$$

$$r_e = \sqrt{(r_a \cos \delta)^2 + (r_b \sin \delta)^2} \quad (21)$$

where $\mu_e = 398600 \text{ km}^3/\text{s}^2$ is the gravitational constant of the earth, $J_2 = 1.08264 \times 10^{-3}$ is the J_2 gravitational constant, $r_a = 6378.135 \text{ km}$ and $r_b = 6356.912 \text{ km}$ are equatorial and polar radiuses of the earth, respectively.

2.4.2. *Atmosphere model.* The US SA76 model is utilized as the atmosphere model. The atmospheric density and temperature are calculated according to the altitude:

$$(\rho, T) = f_{am}(h) \quad (22)$$

where f_{am} is the function to analyze the atmospheric parameters on the basis of the SA76 model.

Then, the sound velocity is given as

$$v_s = 20.0468 \sqrt{T} \quad (23)$$

Furthermore, the Mach number is calculated as:

$$Ma = \frac{v}{v_s} \quad (24)$$

3. Parameterization and discretization of trajectory

The direct shooting method is utilized for parameterization and discretization of the trajectory. First, the continuous time is discretized into a group of time points as follows:

$$t_0 = t_1 < t_2 < \dots < t_N = t_f \quad (25)$$

where t_0 is the initial flight time, t_f is the final flight time, and N is the number of the discretized time points. These time points can be evenly or non-evenly distributed in the time interval $[t_0, t_f]$.

Then, the corresponding discrete control variables are defined as

$$\mathbf{u} = (\mathbf{u}_1, \mathbf{u}_2, \dots, \mathbf{u}_N) \quad (26)$$

In each time interval $[t_i, t_{i+1}]$, the approximate control variables are obtained through linear interpolation:

$$\mathbf{u}(t) = \mathbf{u}_i + \frac{t - t_i}{t_{i+1} - t_i} (\mathbf{u}_{i+1} - \mathbf{u}_i), t_i \leq t \leq t_{i+1}, i = 1, \dots, N - 1 \quad (27)$$

Then, the trajectory has a limited set of state and control variables, which can be calculated and simulated through numerical integration. In addition, as the number of the discrete time points increases, the precision of the numerical calculation rises.

4. Simulation results and comparison

Table 1. Initial values of the state variables

State variable	Initial Value
Altitude /km	12
Ground velocity /(m/s)	236
Flight-path angle /°	5
Azimuth /°	90
Longitude /°	86
Latitude /°	42

Table 2. Comparison on two trajectory parameters

Group	Earth rotation considered ?	Total range /km	Final altitude /km
1	Yes	1069	4
	No	1055	2.9
2	Yes	985	3
	No	967	2.5

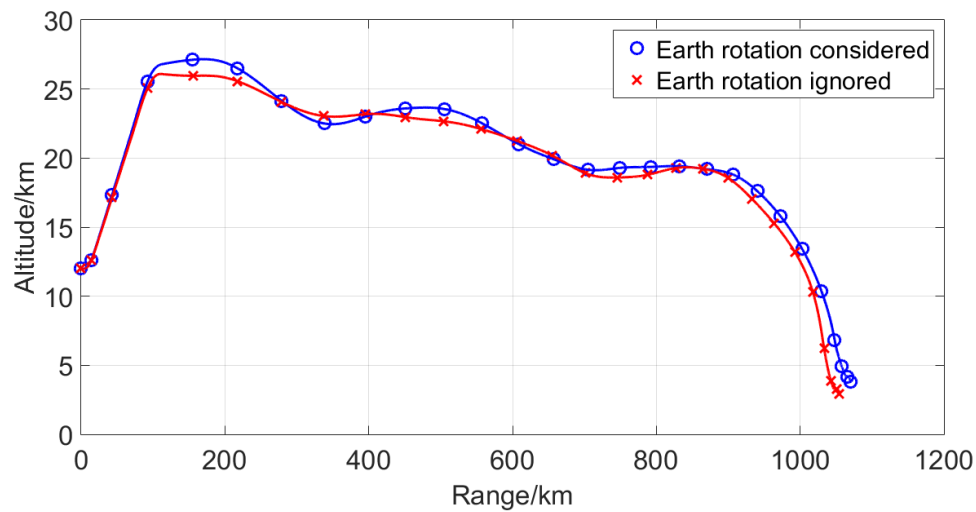


Figure 1. Comparison on trajectories in 1st group.

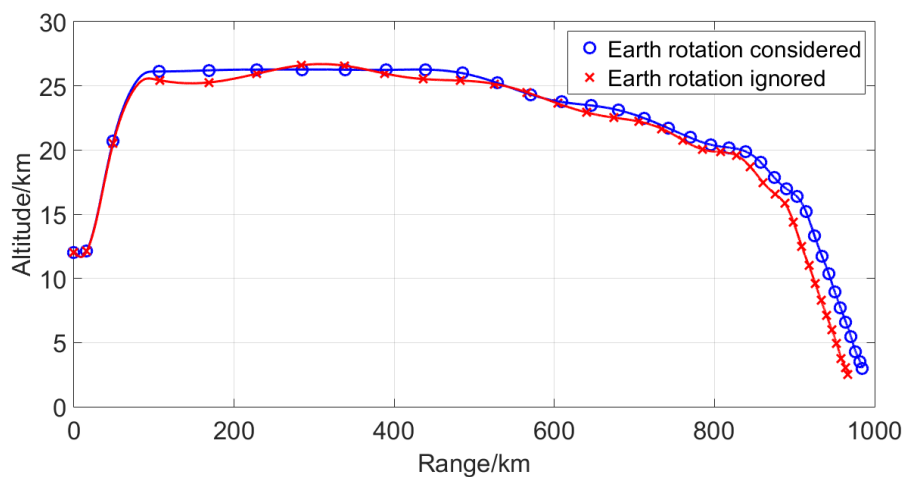


Figure 2. Comparison on trajectories in 2nd group.

In this paper, two groups of trajectory simulation are implemented. It is worth noting that the trajectory is only simulated till the start of approach and landing phase.

In each group, the initial state, the control variable as well as input parameters which includes engine, mass and aerodynamic parameters are all the same. The only difference is whether the earth rotation is considered. In addition, in each simulation, initial values of the state variables are set in table 1. Then, the two groups of results are depicted in figure 1 and figure 2, respectively. The comparison on the total range as well as the final altitude is made in table 2.

It is inferred from the results that the two trajectories in each group are different with each other. When the earth rotation is ignored, the total range is shortened by about 15 ~ 20 km with a percentage of 2%. The distance reduction approximately equals the whole range of approach and landing phase. Meanwhile, the final altitude decreases about 0.5 ~ 1 km with a relatively large percentage of 15% ~ 25%. Both of these two points may deteriorate the control precision of the unpowered approach and landing flight and may make the final landing fail. As high accuracy is needed for a returnable hypersonic cruise vehicle during the unpowered return flight, it is suggested to take the earth rotation into consideration in order to improve the accuracy of the trajectory simulation and mission analysis.

5. Conclusion

In this paper, the dynamic equations for a hypersonic cruise vehicle are derived, in which the earth rotation is taken into account. The direct shooting method is used for parameterization and discretization of the trajectory. Afterward, based on two groups of trajectories obtained through numerical simulation, the trajectory with the earth rotation included is compared with that without the rotation in each group. It is shown that the earth rotation has effects on the flight range as well as the final altitude. As high accuracy and precision is needed for a returnable hypersonic cruise vehicle, especially in the final unpowered return flight, it is suggested to involve the earth rotation in order to improve the accuracy of the mission analysis and control subsystem design.

Acknowledgments

This work is supported by grants from the Natural Science Foundation of China (NSFC 61403028).

References

- [1] Marc A B 2004 *Performance Study of Two-Stage-To-Orbit Reusable Launch Vehicle Propulsion Alternatives* (Ohio: Air Force Institute of Technology Press) p 12–19
- [2] McClinton C R, Rausch V L, Nguyen L T and Sitz J R 2005 Preliminary X-43 flight test results *Acta Astronautica*. **57** 266–276
- [3] Roh W and Kim Y 2002 Trajectory optimization for a multi-stage launch vehicle using time finite element and direct collocation methods *Engineering Optimization*. **34** 15–32
- [4] Grant M J and Braun R D 2015 Rapid indirect trajectory optimization for conceptual design of hypersonic missions *J. Spacecraft and Rockets*. **52** 177–182
- [5] Manickavasagam M, Sarkar A K and Vaithyanathan V 2015 Trajectory optimisation of long range and air-to-air tactical flight vehicles *Defence Science Journal*. **65** 107–118
- [6] Zhao J and Zhou R 2013 Reentry trajectory optimization for hypersonic vehicle satisfying complex constraints *Chinese Journal of Aeronautics*. **26** 1544–53
- [7] Liu X and Shen Z 2016 Entry trajectory optimization by second-order cone programming *J. Guidance, Control, and Dynamics*. **39** 227–241
- [8] Li Z, Hu C, Ding C, Liu G and He B 2018 Stochastic gradient particle swarm optimization based entry trajectory rapid planning for hypersonic glide vehicles *Aerospace Science and Technology*. **76** 176–186
- [9] Rahimi A, Kumar K D and Alighanbari H 2013 Particle swarm optimization applied to spacecraft reentry trajectory *J. Guidance, Control, and Dynamics*. **36** 307–310